Available online at www.sciencedirect.com
ScienceDirect
Carbohydrate Polymers 74 (2008) 170–184
Carbohydrate Polymers
www.elsevier.com/locate/carbpol

Physicochemical properties of etherified maize starches

Annemarie M.L. Huijbrechts [a,b,*,2], Melinda Desse [c,2], Tatiana Budtova [c,2], Maurice C.R. Franssen [a], Gerben M. Visser [a], Carmen G. Boeriu [b,2], Ernst J.R. Sudhölter [a,1]

[a] *Laboratory of Organic Chemistry, Agrotechnology and Food Sciences Group, Wageningen University, Dreijenplein 8, 6703 HB Wageningen, The Netherlands*
[b] *Division of Biobased Products, Agrotechnology and Food Sciences Group, Bornsesteeg 59, 6708 PD Wageningen, The Netherlands*
[c] *Ecole des Mines de Paris, Centre de Mise en Forme des Matériaux, UMR CNRS/Ecole des Mines de Paris 7635, BP 207,06904 Sophis-Antipolis, France*

Received 4 December 2007; received in revised form 28 January 2008; accepted 4 February 2008
Available online 14 February 2008

Abstract

The changes in starch properties due to etherification with allyl glycidyl ether (AGE) have been investigated. After etherification of three different starches (containing 0.9%, 27% and 70% amylose), no appreciable differences in granular appearance were observed, but the granule crystallinity of these starches was changed. Furthermore, the incorporation of AGE in the starch significantly affects its physicochemical properties: the gelatinization temperatures were decreased and the pasting properties were altered. Both the swelling power and the solubility index increased as the degree of substitution (DS) increased. The rheology behaviour of the droplets of swollen granules suspension was studied under shear flow conditions.

Keywords: Etherification of maize starch; Granule morphology; Pasting properties; Rheological properties; Swelling power; Gelatinization

1. Introduction

Starch and its derivatives are of interest for food and non-food applications e.g. in paper, textile and pharmaceuticals. However, the uses of starch are often limited by unfavourable properties, such as low solubility in water, the tendency of retrogradation etc., depending upon the application (Rutenberg & Solarek, 1984). To extend their applications, functional groups can be introduced into starches by a number of chemical or physical modifications in order to provide starches with improved or specific properties. Modified starches generally have markedly altered physicochemical properties, compared to their native starches, depending on the degree of substitution and the type of functional groups introduced (Rutenberg & Solarek, 1984). Starch ethers, i.e. hydroxypropylated (Liu, Ramsden, & Corke, 1999), allylated (Bhuniya, Rahman, Satyanand, Gharia, & Dave, 2003; Kondo, Isogai, Ishizu, & Nakano, 1987; Nicohols, Hamilton, Smith, & Yanovsky, 1945; Nud'ga, Petrova & Lebedeva, 2003; Tsai & Meier, 1990; Wilham, McGuire, Rudolfhi, & Mehltretter, 1963) and methallylated starches (Kondo et al., 1987), comprise a wide range of industrial products of different degree of substitution and useful physiochemical properties. For example, the introduction of hydroxypropyl group in maize starches weakens the bond strength between starch molecules and thereby increases the swelling power and the solubility of the starch granule upon heating (Liu, Ramsden, et al., 1999).

In previous studies (Nicohols et al., 1945; Wilham et al., 1963), it was found that after air exposure allylated starch exhibited a gummy texture, coated with hard insoluble material, due to cross-linking polymerization caused by oxidation. These properties afford possibilities for applica-

* Corresponding author. Tel.: +31 317 482369; fax: +31 317 484914.
E-mail address: Annemarie.Huijbrechts@wur.nl (A.M.L. Huijbrechts).
[1] Present address: Delft University of Technology, Department of DelftChemTech, Laboratory of Nano-organic chemistry, Julialaan 136, 2628 BL Delft, The Netherlands.
[2] Members of the European Polysaccharide Network of Excellence (EPNOE), www.epnoe.eu.

0144-8617/$ - see front matter © 2008 Elsevier Ltd. All rights reserved.
doi:10.1016/j.carbpol.2008.02.001

tion in protective and decorative coatings for wood, glass, metal and other surfaces, for coating and impregnating paper and textiles and for the preparation of laminated products or rigid plastics. Alternatively, hydrogels could be prepared by allyl-starch copolymerised with methacrylic acid itself and/or its combination with acrylamide. These starch-based hydrogels appeared to have high water absorption capacity, enhanced biodegradability, improved bioadhesive properties and faster drug release (Ameye et al., 2002; Bhuniya et al., 2003). Other graft allylated polymers are used as additives in paper making and for thermoplastic and biocompatible materials (Nud'ga et al., 2003; Tsai & Meier, 1990).

Previously, we reported on a new synthetic route towards 1-allyloxy-2-hydroxy-propyl-starch (AHP-starch) using allyl glycidyl ether under mild reaction conditions (Huijbrechts et al., 2007). Using chemical characterization methods, differences in molecular structures of the modified and native starch were obtained. However, very little information is available on the granular structure, physical and chemical properties of these kinds of modified maize starches. The aim of this paper is to study the effect of AHP groups on waxy, normal and amylose-enriched maize starch, which have reacted with allyl glycidyl ether under mildly alkaline conditions. The thermal and pasting properties, swelling power and solubility index, granule morphology and flow behaviour under shear are studied.

2. Materials and methods

2.1. Starch samples

Amylose-enriched maize starch (70% amylose, AEMS), maize starch (27% amylose, MS) and waxy maize starch (0.9% amylose, WMS) were purchased from Tate & Lyle (The Netherlands). Allyl glycidyl ether (AGE) was obtained from Sigma–Aldrich Chemie B.V. (The Netherlands). Polydimethylsiloxane Rhodorsil 47V 200 000 (PDMS) with viscosity of 220 Pa s was provided by Rhodia, France.

2.2. Synthesis of AHP-starch

1-Allyloxy-2-hydroxy-propyl-starches (AHP-starch) were prepared according to the method described earlier (Huijbrechts et al., 2007) with slight modifications. A range of different degrees of substitution were obtained by adjusting the reaction conditions as follows: Starch was suspended in distilled water to a slurry of 200 or 400 g/kg. NaOH (1.5% or 4% mol/mol dry starch) and Na_2SO_4 (5% or 35% g/g dry starch) were added to the mixture which was heated to 48 °C, after which allyl glycidyl ether (0.1625 or 1.66 g/g dry starch) was added. The products were isolated as previously described (Huijbrechts et al., 2007). The degree of substitution of AHP-starches was determined by ^{1}H NMR using the equation presented in previous study (Huijbrechts et al., 2007). A Karl Fisher titration is used to determine the moisture content of the starch compounds as described in the previous paper (Huijbrechts et al., 2007).

2.3. Scanning electron microscopy

Scanning electron microscopy micrographs were obtained on a JEOL JSM-6300 scanning electron microscope. The samples were attached to circular silver stubs with double-sided tape on a carbon tape and coated by platinum sputtering using a Jeol JFC-1200 fine coater (Tokyo, Japan). 'Air-dry' samples were viewed by scanning the total specimen and a representative area was photographed at a magnification up to 6000×.

2.4. X-ray diffraction patterns

The X-ray diffraction measurements were performed on a Panalytical X'Pert Pro diffractometer (Panalytical, Almelo, The Netherlands) using nickel-filtered CuKα radiation (tube operating at 40 kV and 40 mA). The data were collected by using an automatic divergence slit (5 mm irradiated length) and a 0.2 mm receiving slit with dry starch under N_2 atmosphere. The scanning regions were collected from 7° to 30° (2θ) in step size of 0.02 (2θ). The degree of crystallinity (DC) of the samples was calculated by comparing the diffraction patterns of the samples with that of an amorphous waxy maize sample (Cairns, Bogracheva, Ring, Hedley, & Morris, 1997; Tan, Flanagan, Halley, Whittaker, & Gidley, 2007).

Sample preparation. A standard amorphous waxy maize starch was prepared by heating a 10.7% suspension (w/w) for 1 h at 95 °C followed by drying under vacuum conditions at 60 °C for 48 h. The dried gelatinized starch sample was then crushed to obtain amorphous starch powder. The X-ray diffraction analyses of this amorphous sample gave a typical broad "amorphous" halo, indicating the absence of crystalline structure in these samples (Tan et al., 2007). The other samples are crushed under N_2 atmosphere and kept in a desiccator over KOH pellets for one week. The water content of all samples were adjusted via equilibration in a desiccator for one week over saturated K_2CO_3 salt solution at 20 °C, providing a relative humidity (RH) of 44% ($a_w = 0.44$) (Cairns et al., 1997).

2.5. Differential Scanning Calorimetry

The temperature of gelatinization was measured using a Differential Scanning Calorimeter (Perkin Elmer DSC-7, Boston, USA). Starch (8.5 mg) was weighed into a 40-μl capacity stainless steel pan (Mettler-Toledo, Switzerland) and distilled water was added with a microsyringe to achieve a suspension with a starch–water ratio of 1:4 (w/w). The pans were hermetically sealed and allowed to stand for 24 h at room temperature before heating in the DSC (Radosta et al., 2004). An empty steel pan was used as a reference. Sample pans were heated at a rate of 5 °C/min

from 20 °C to 150 °C. The PE Pyris – DSC-7 software was used for data handling. Onset temperature (T_o), peak temperature (T_p), final temperature (T_c) and enthalpy of gelatinization (ΔH_{gel}) were calculated as described in the literature (Altay & Gunasekaran, 2006). ΔH_{gel} was based on the dry material (J/g dry starch).

2.6. Rapid Visco-Analyser

The pasting properties of starch samples were determined using a Rapid Visco-Analyser-4 (RVA) (Newport Scientific Pvt. Ltd., Warriewood, Australia). Starch (3.0 g dry base) and a weighed amount of distilled water were mixed and stirred in the aluminium RVA sample canister to make a 10.7% starch suspension (w/w). A programmed heating and cooling cycle was used, where the sample was stirred rapidly at 960 rpm for 10 s and was held at 50 °C for 1 min. In the next steps, the shear input was decreased to 160 rpm and held constant. The sample was heated to 95 °C in 7.5 min, held at 95 °C for 5 min, cooled to 50 °C in 8.5 min and then held at 50 °C for 3 min (Liu, Ramsden, et al., 1999). Triplicate tests were performed in each case. Pasting onset (P_{onset}), pasting temperature (P_{temp}), peak viscosity, trough or hot paste viscosity, final or cool paste viscosity, breakdown (peak minus hot paste viscosity) and setback (final minus hot paste viscosity) were recorded or calculated (Ji et al., 2003).

2.7. Swelling power and solubility index

The swelling power of starches was determined via a method adapted from the literature (Subramanian, Hoseney, & Bramel-Cox, 1994). Starch (0.1 g dry base) was mixed in 2 ml distilled H_2O for 4 h at 60 °C. The mixture was centrifuged at 15,000 rpm for 15 min. The supernatant was decanted and the wet starch sediment was weighed. Swelling power is defined as the ratio of the weight of the wet sediment to the initial weight of dry starch. The solvent of the supernatant was evaporated at 100 °C for 4 h. The solubility index was determined from the ratio of the weight of the dried supernatant to initial weight of the dry starch. The experiment was repeated three times and the mean values are reported.

2.8. Dimension of granules and microscopic observations

The dimension of the granules was obtained using a hot stage microscope Olympus BX60 (Olympus Nederland BV, The Netherlands) connected with a Linkam PE94 heat controller (Linkam scientific instruments, UK) and an EHEIM DB IP44 water bath, at a magnification of 20× and 50×. After the heating process (as used for the swelling power and solubility) and cooling to room temperature, suspensions of unmodified starches and modified starches were put onto object glasses, covered with cover glasses and observed using the light microscope. Photos were taken using an Olympus D70 camera (Olympus Nederland BV, The Netherlands) and stored in a PC. Photos were further treated, for improving their image, using the analySIS Image Processing software (Olympus Nederland BV, The Netherlands). With ImageJ (Rasband, 1997–2006), the average area was calculated after converting pixels to μm by means of known reference lengths. For these size measurements, more than 100 granules were used from different photos and samples. The outline of the granules was fainter for the modified starches than unmodified starches.

2.9. Rheology

Steady shear experiments were carried out at 20 °C using a plate–plate geometry (plate diameter 40 mm, gap of 700 or 1000 μm) on a stress-controlled Bohlin Gemini® rheometer (Malvern, UK) equipped with a Peltier temperature control system. Shear rates were varied from 0.1 to 50 s^{-1}. The suspensions of starch granules swollen to their maximum with 100% volume fraction were prepared taking into account the swelling power of each sample determined previously. Dry starch was mixed with water in such proportions that after the heating/cooling cycle there was no free water around the granules and they were swollen to maximal swelling power. The heating/cooling cycle was as follows: suspensions of MS and WMS and their modified counterparts were first heated to 60 °C, kept for 30 min and then cooled to 20 °C. These suspensions were used for performing the rheological and rheo-optical measurements.

2.10. Rheo-optics

A transparent counter-rotating shear cell (Vervoort & Budtova, 2005; Zanina & Budtova, 2002) was used to observe the behaviour of a droplet of starch suspension under simple shear (Fig. 1). A droplet of starch suspension with 100% granules volume fraction was placed in PDMS which was chosen as being inert, transparent, Newtonian (in the interval of shear rates used), sufficiently viscous to exert rather high shear stresses and immiscible with aqueous systems thus allowing good visualization of deforming aqueous droplets (Vervoort & Budtova, 2005; Zanina & Budtova, 2002)

Both transparent plates (see Fig. 1) rotate in opposite directions; data on geometry and flow characteristics are stored in a computer. An optical microscope placed under one of the rotating plates allows observations in the plane formed by the flow direction and the vorticity axis. All experiments were recorded by a CCD camera coupled to a time-coding system and linked to a DVD recorder and a monitor. By adjusting the relative velocities of the plates, a selected object can be immobilized in the laboratory framework and its behaviour can be monitored.

The system PDMS with starch suspension to be placed between the plates was prepared as follows. An adequate volume of polydimethylsiloxane PDMS was placed on the lower plate. A droplet of suspension of swollen starch granules was placed on the top of PDMS and covered with

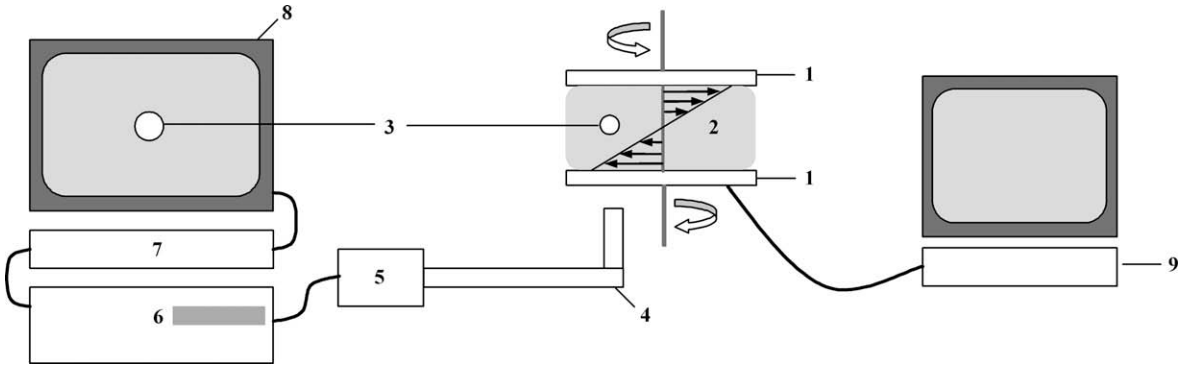

Fig. 1. Schematic representation of the counter-rotating rheo-optical setup: transparent plates (1), suspending fluid PDMS (2), droplet of the suspension of swollen starch particle (3), optical microscope (4), CCD camera (5), video recorder (6), time-coding system (7), monitor (8) and computer system (9).

another layer of PDMS. Before setting the gap (900 μm), the system was let to rest for air bubbles to disappear. During each experiment, the system was submitted from low to higher shear stresses by increasing the rotation velocities of the plates. All the experiments were performed at room temperature.

3. Results and discussion

3.1. Granule morphology of AHP-starch

Three types of starch (WMS, MS and AEMS) were treated with allyl glycidyl ether as described before (Huijbrechts et al., 2007) and their physicochemical properties were compared to the native starches. The granule appearance of the dry starch samples was investigated using scanning electron microscopy (SEM) (Fig. 2). The appearance of WMS is characterised by its distinct granules, having polygonal shapes, which have irregular or porous surfaces (Fig. 2A). The MS granules show cubical and more spherical shapes having some smooth and some porous surfaces (Fig. 2B), while AEMS granules appear as smooth and uniform, with some elongated granules (Fig. 2C). As in previous studies (Chen, Yu, Chen, & Li, 2006; Li, Vasanthan, Hoover, & Rossnagel, 2004), the shape of granular appearance is more polygonal for amylopectin-rich starches than the amylose-rich starches, but the surfaces of the amylose-rich starches are smoother than those of the amylopectin-rich starches. The granules of AHP-WMS, AHP-MS and AHP-AEMS show similar size and appearance. (Fig. 2D, E and F). However, comparing the micrographs at 6000× (not shown) shows that the surface of the granule from AHP-WMS and AHP-MS is rougher and more porous as compared to native WMS and MS. The SEM image of AHP-AEMS show smooth granules with small amount of exudates around them. Leaching of amylose at lower temperature after AHP substitution might produce this appearance of exudates. It is reported that leaching of a

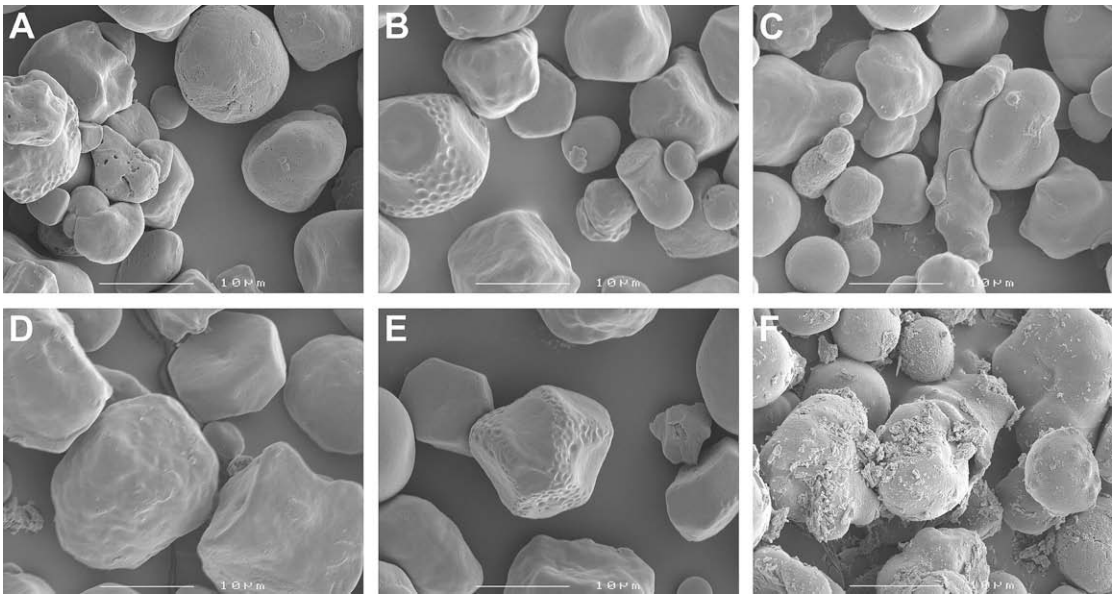

Fig. 2. SEM-images of (A) WMS, (B) MS, (C) AEMS, (D) AHP-WMS (DS 0.23), (E) AHP-MS (DS 0.11) and (F) AHP-AEMS (DS 0.13). The micrographs (A–F) were taken at 3000× magnification.

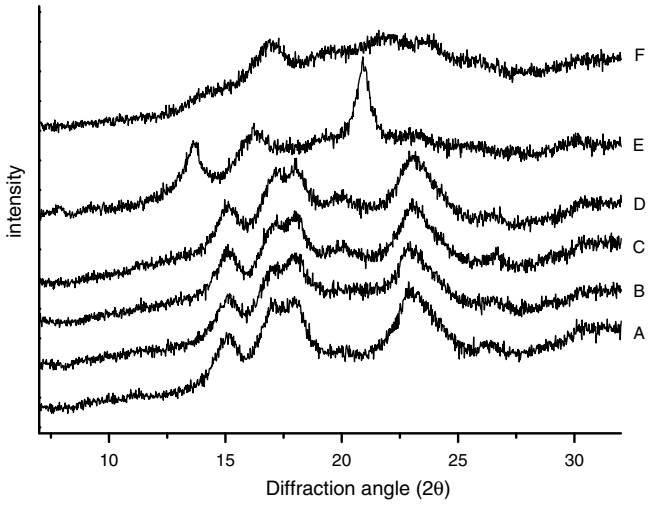

Fig. 3. X-ray diffractograms of (A) WMS, (B) AHP-WMS (DS = 0.23), (C) MS, (D) AHP-MS (0.11), (E) AEMS and (F) AHP-AEMS (DS = 0.13).

small amount of exudates occurred at 55 °C for high amylose starch (Li et al., 2004).

The results obtained suggest that chemical etherification of WMS, MS and AEMS does not induce significant changes in the shape of the starch granules. Only minor surface modification may occur upon reaction, resulting in a slightly rougher and more porous surface, and a small amount of exudates.

3.2. X-diffraction pattern of modified maize starches

Using X-ray diffraction, information on the starch granule crystallinity was obtained. The X-ray diffraction patterns and crystallinity of waxy, normal and high amylose maize starch show that the degree of crystallinity (DC) decreases with the increase in amylose content (Fig. 3 and Table 1) which is in agreement with reported data (Cheetham & Tao, 1998; Gernat, Radosta, Anger, & Damaschun, 1993). WMS and MS show a typical A-type pattern with strong reflections at 2θ of about 15°, 17°, 18° and 23°. The X-ray diffraction pattern of AEMS has a typical B-type with a strong peak around 17° and small peaks at 20°, 22° and 23°. The additional effect of the substitution on the starch crystallinity is shown in Fig. 3 and Table 1. AHP-WMS and AHP-MS starch show similar X-ray diffractograms as their native form. However, a significant decrease of DC was observed, namely 12.4% for AHP-WMS and 16.8% for AHP-MS, respectively. There was no significant difference in DC between native AEMS and AHP-AEMS. However, their X-ray diffraction patterns are different from each other. The X-ray diffraction pattern of AHP-AEMS has two decreased peaks at 17° and at ~22°, and all peaks shifted to higher 2θ. This observation might indicate that the molecular structure in AHP-AEMS is changed or disappeared, with subsequent rearrangement to another ordered crystal structure that is close to V-type.

In previous studies (Lewandowicz, Fornal, & Voelkel, 2001; Wang & Wang, 2002), modified starch with a high level (DS > 0.1) of cationic groups showed also a significant decreased crystallinity. However, starch substituted with a low level of cationisation or acetylation (DS < 0.1) revealed no substantial changes in the of X-ray diffraction pattern and crystal structures.

Summarising, with AHP substitution, no substantial differences in X-ray diffraction pattern for WMS and MS is obtained. The crystallinity level is changed, although the shapes of starch granules remain almost unaltered.

3.3. Thermal properties

The DSC thermograms obtained during heating of different aqueous maize starch dispersions are presented in Fig. 4. The thermograms of all compounds show the endothermic transitions, which are typical for starch. Enthalpy is the latent heat absorbed by melting of crystallites in the granules, it depends on a number of factors like crystallinity, intermolecular bonding, rate of heating of the starch suspension, presence of other chemicals, etc. (Moorthy, 2007). Usually the low temperature endothermic transition is ascribed to amylopectin double helix dissociation and the melting of the crystalline lamellae, while the high temperature transition is mainly attributed to the dissociation of the amylose–lipid complexes (Matveev et al., 2001; Rolee, Chiotelli, & Meste, 2002). This explains the almost complete absence of the second transition for low amylose containing starch such as WMS. The starch with high amylose contents gelatinizes at a high temperature because of the

Table 1
X-ray diffraction data of native and AHP-starches

Sample	DS	2θ values (° angle)						DC[a] (%)
		23°	22°	20°	18°	17°	15°	
WMS		22.84		20.06	18.18	17.07	15.16	41.9
AHP-WMS	0.23	22.84		20.04	17.92	17.12	15.15	29.5
MS		23.06		20.00	18.00	17.18	15.15	38.9
AHP-MS	0.11	23.02		19.95	18.00	17.23	15.12	22.1
AEMS		23.11	20.91	19.09		16.25		17.5
AHP-AEMS	0.13	23.64	21.95	19.49		16.92		21.5

[a] Degree of crystallinity.

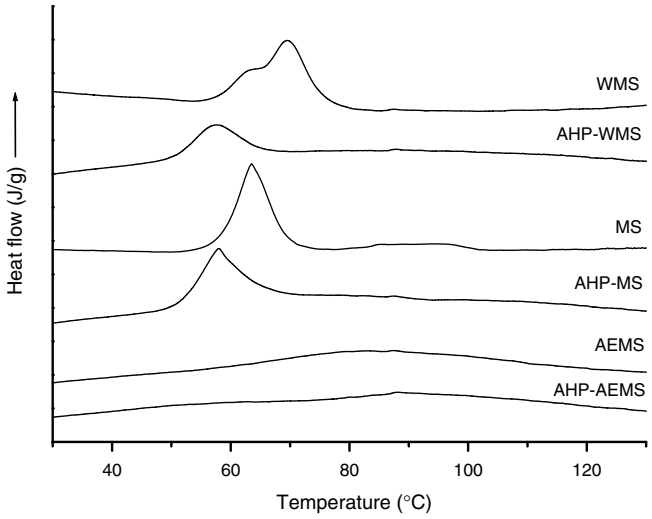

Fig. 4. Differential Scanning Calorimetry thermograms of native and AHP-starches: WMS, AHP-WMS (DS = 0.23), MS, AHP-MS (DS = 0.11), AEMS and AHP-AEMS (DS = 0.13).

presence of amylose–lipid complex, but needs a lower enthalpy and vice-versa, i.e. starch with low amylose content gelatinized at a low temperature and uses a higher enthalpy (Table 2) (Kaur, Singh, & Singh, 2004). Besides the differences of amylose contents in starch, all AHP substituted starches show decreased gelatinization temperatures, while AHP-WMS and AHP-MS show a decreased gelatinization enthalpy (Table 2). A low ΔH_{gel} suggests a lower percentage of organized arrangements or a lower stability of the crystals (Kaur et al., 2004). These differences may be ascribed to the influence of AHP group on the interactions between the starch chains, through steric hindrance by the AHP group, change of hydrophilicity of the starch, or interactions of the hydroxyl group of AHP group with starch chains. Decreases in the thermal parameters are consistent with fewer crystals being present after etherification and with a cooperative melting process enhanced by additional swelling (Jenkins & Donald, 1998; Kaur et al., 2004; Liu, Ramsden, et al., 1999). A decrease was recorded for the transition temperatures and

Table 2
Thermal properties of native and AHP-starches during heating[a]

Sample	DS	Gelatinization temperature (°C)			ΔH_{gel} (J/g)[b]
		T_o[c]	T_p[d]	T_c[e]	
WMS		57.0	69.5	75.9	13.1
AHP-WMS	0.23	50.8	57.3	65.9	4.9
MS		58.5	63.5	69.3	8.9
AHP-MS	0.11	51.4	58.1	67.5	7.9
AEMS		72.7	88.2	115.0	4.5
AHP-AEMS	0.13	59.9	83.5	110.8	7.8

[a] Measured in Differential Scanning Calorimeter.
[b] ΔH_{gel} = enthalpy of gelatinization.
[c] T_o = onset temperature.
[d] T_p = peak temperature.
[e] T_c = final temperature.

ΔH_{gel} of all AHP substituted starches, except for AHP-AEMS (Table 2). ΔH_{gel} has slightly increased for AHP-AEMS, which could indicate the better molecular order within the granule after AHP substitution. It suggests that AHP substitution in AEMS induces a more ordered orientation of the starch molecules with the granule, although the starch granules are disrupted at slightly lower gelatinization temperatures.

All AHP-starches gelatinizes at lower temperature accompanied with a change in ΔH_{gel}. Variations in enthalpy of substituted starches are indications of structural divergence: molecular structure (amylose and amylopectin fine structures, distribution pattern of AHP groups) and composition (amylose-to-amylopectin ratio, DS) (Donald, 2007).

3.4. Pasting properties

Pasting viscosity profiles of starches analyzed using Rapid Visco-Analyser (RVA) are shown in Fig. 5 and the results are summarized in Table 3. Pasting of starch is a phenomenon following gelatinization in the dissolution of starch. It involves granular swelling, exudation of molecular components from the granule and eventually, total disruption of the granules (Atwell, Hood, Lineback, Varriano-Marston, & Zobel, 1988; Thomas & Atwell, 1999). The pasting properties of starch are affected by the amylose and lipid contents and by branch chain-length distribution of amylopectin. Amylopectin contributes to swelling of starch granules and pasting, whereas amylose and lipids inhibit the swelling (Atwell et al., 1988; Tester & Morrison, 1990; Whistler & Bemiller, 1997).

The RVA results show that the onset pasting temperatures (P_{onset}), i.e. the temperature at which a perceptible increase in viscosity occurs (Ji et al., 2003; Moorthy, 2007), of modified and unmodified starches, are higher than the onset gelatinization temperatures (T_o), determined by DSC, i.e. the temperature at which the starch granules gelatinized. ΔT ($P_{onset} - T_o$) for the native starches is for WMS $\approx$ 12 °C, for MS $\approx$ 16 °C. For AEMS, ΔT could not be determined, while for the AHP substituted WMS, MS and AEMS is, respectively, $\approx$5 °C, $\approx$12 °C and $\approx$34 °C. Thus, the differences between T_o and P_{onset} decreases after substitution. This suggests that the gelatinization and the increase in viscosity occurred at a shorter temperature range for AHP substituted starches than for their non-modified starches. Furthermore, the shapes of the pasting curves differed markedly after etherification. All AHP-starches results in an increased setback, indicating that retrogradation takes places, i.e. a process in which molecules comprising gelatinized starch starts to reassociate in an ordered structure (Atwell et al., 1988). It is reported in the literature that waxy maize starch has a lower pasting temperature, a higher peak viscosity and lower setback than maize starch (Tester & Morrison, 1990). In general, the setback reflects the gel network formation involving amylose which is very low for WMS,

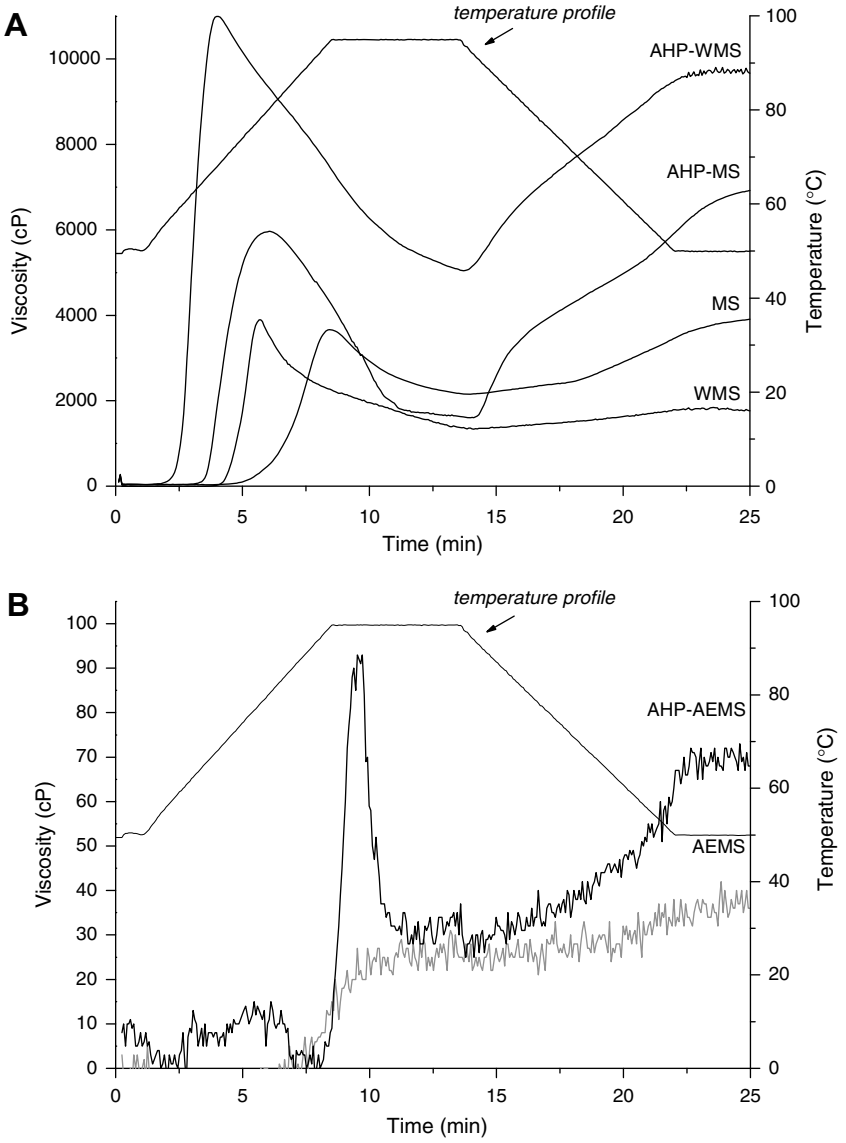

Fig. 5. RVA pasting profiles of native and AHP-starches: (A) WMS, AHP-WMS (DS = 0.23), MS and AHP-MS (DS = 0.11) (B) AEMS and AHP-AEMS (DS = 0.13).

Table 3
Pasting properties of native and AHP-starches[a]

Sample	DS	P_{onset}[b] (°C)	P_{temp}[c] (°C)	Viscosity (cP)				
				Peak	Hot paste	Final paste	Breakdown[d]	Setback[e]
WMS	–	68.5	78.3	3934	1637	1826	2297	189
AHP-WMS	0.23	55.5	68.0	10841	5402	9647	5439	4245
MS	–	74.9	94.7	3648	2188	3950	1460	1762
AHP-MS	0.11	63.7	80.8	5885	1891	7097	3994	5206
AEMS	–	–	–	–	–	36	–	36
AHP-AEMS	0.13	94.1	95.0	74	–	64	10	64

[a] Measured in Rapid Visco-Analyser.
[b] P_{onset} = pasting onset.
[c] P_{temp} = pasting temperature.
[d] Peak viscosity minus hot paste viscosity.
[e] Final paste viscosity minus hot paste viscosity.

and that is indeed what we observed (Jane et al., 1999) (Table 3). AHP-WMS show a higher peak viscosity, higher breakdown, higher setback and a higher final paste viscosity than its native starch. A similar but smaller effect has been obtained for the differences in MS and AHP-MS. A large swelling of the granule can lead to an increased peak

viscosity (Liu, Ramsden, et al., 1999). Presumably, the substitution induces less ability to withstand heating and shear stress and, therefore, the breakdown increases. The higher setbacks, which were obtained, suggest that the tendency for recrystallization is increased for AHP-WMS and AHP-MS. Thus, the ability to form a viscous paste is increased when the starches are etherified. The final paste viscosity of the AHP substituted starch is higher than the native starches and that means the materials forms a better gel after cooling than the native starches. These differences may be ascribed to the structural changes of starch granules taking place during the reaction conditions used (Liu, Ramsden, et al., 1999).

Because of a high amylose content in AEMS, the starch hardly shows any swelling (Jane et al., 1999), and, thus, displays very low viscosity as shown in Fig. 5B. The substituted AEMS induces a low peak viscosity, low breakdown and low setback. The gelatinization is initiated at lower temperature, and AHP-AEMS is prone to swelling. The swelling of granules leads to a small peak viscosity. The setback and breakdown are similar to the peak viscosity, which means the formation of gel network did not seem to occur in this modified starch.

3.5. Swelling and solubility index versus degree of substitution

The swelling power and solubility index is dependent on the starch species, and on the type and extent of modification (Bhandari & Singhal, 2002). During heating, water penetrates into the more accessible amorphous region of the granule, resulting in hydration and limited swelling. At the gelatinization temperature, the swelling of the amorphous phase (water-penetrated phase) accelerates the disruption of the crystalline region. This development can be ascribed to the swelling power of the starch granules. The swelling power of all AHP-starches increases as substitution increases (Fig. 6). AHP-WMS shows the highest increasing swelling power as the DS increases. The lowest increased swelling power is for AHP-AEMS due to the high amylose content, and its high gelatinization temperatures. The incorporation of allyl glycidyl groups seems to reduce the interactions between molecules of starch inducing the increase of hydrophilicity of starch, i.e. the incorporation of substitution changes the polymer–solvent interaction causing lower gelatinization temperatures (described by DSC) and increases swelling power. In previous studies on hydroxypropylated (Liu, Ramsden, et al., 1999), carboxymethylated (Fadzlina, Karim, & Teng, 2005) and acetylated starch (Shon & Yoo, 2006), an analogous tendency of increased swelling power with increased substitution is observed.

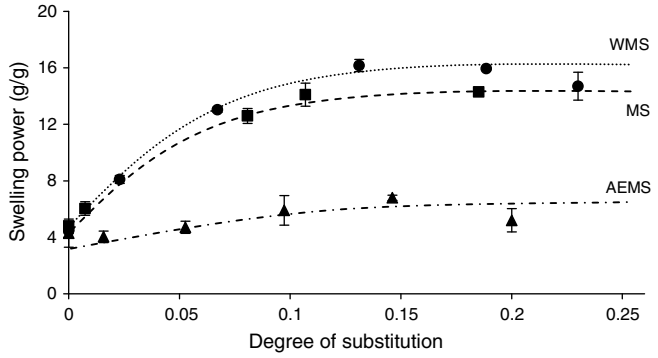

Fig. 6. Swelling power of native and AHP-maize starches at 60 °C. The lines are given to guide the eye; dotted, dashed and dashed-dotted lines correspond to modified ●, WMS; ■, MS and ▲, AEMS, respectively.

The solubility index of the native and modified starches was also studied as a function of DS. The solubility is associated with the hydrophilicity and ease of disruption of the starch granules. AHP-WMS and AHP-MS showed an increased solubility upon substitution (Fig. 7). Due to the high content of crystalline amylopectin, the modified WMS shows a lower increased solubility for an increasing DS than for AHP-MS. A similar effect for acetylated WMS, MS and AEMS was described in other substituted starch studies (Liu, Corke, & Ramsden, 1999; Liu, Ramsden, & Corke, 1997). AEMS has the lowest increase of the solubility index when the substitution increases, due to its high amylose content and its gelatinization temperatures.

The swelling power and solubility index of all starches seems to go to a saturation limit. This tendency was observed also for other substituted starches (Bhandari & Singhal, 2002; Fadzlina et al., 2005; Liu et al., 1997; Shon & Yoo, 2006). The question is whether this saturation limit is due to the distribution pattern of AHP groups, or to the degree of substitution. The purpose was to measure the relatively swelling capacity and the amount of soluble material for starch granules at a certain temperature. We know from the previous study (Huijbrechts et al., 2007) that the amorphous region in the starch granule is more substituted than the crystalline region. Because of the AHP substitution in the amorphous region, greater water uptake is permitted resulting in an increase in the swelling of the granule. Furthermore, the swelling capacity for the AHP-starches, depending on the substitution, could already be high at room temperature compared to the maximum swelling capacity of the native starches. Based on this information, we assume that small differences in swelling capacity for modified starches may be induced at higher temperature, due to the already high swelling capacity at room temperature. A similar suggestion was made in the study to carboxymethylated starch, which had a swelling capacity at room temperature between 60% to 80% of the maximum swelling capacity for the native starch at 95 °C (Fadzlina et al., 2005). Consequently, a saturation limit for the swelling power and the solubility index for modified starch at a certain temperature might be approached, depending on the substitution. Other properties such as gelatinization temperature and viscosity of the different starches modified with different residues, related to swelling and solubility of starch granules could be investigated to elucidate this tendency.

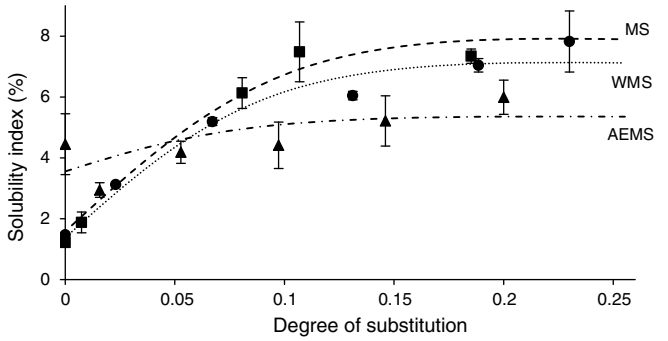

Fig. 7. Solubility index of native and AHP-maize starches at 60 °C. The lines are given to guide the eye; dotted, dashed and dashed-dotted lines correspond to modified ●, WMS; ■, MS and ▲, AEMS, respectively.

In general, increased DS leads to increased swelling power, which indicates a more rapid hydration of the modified starch granule than its native starch. A higher accessibility of the amorphous regions of the starches contributes to an increase of the solubility index, as is observed for the waxy and normal maize starch derivatives.

3.6. Particle dimension of swollen granules

It is known from the literature (Chen, Yu, Kealy, Chen, & Li, 2007) that the granule area increases in the order AEMS-MS-WMS within an certain temperature range. When the starch granule is heated, the growth of starch granules is controlled by two factors: swelling and dissolution. Most of the granules remain intact below their destruction temperature (T_c in DSC measurements, Table 2) (Chen et al., 2007; Tester & Morrison, 1990). Therefore, the area distribution of all the granules heated at 60 °C was studied using a hot stage microscope and the results are illustrated in Table 4 and Fig. 8 for native starches and AHP substituted starches.

The results show that the substitution of three different starches has considerable influence on the area distribution of their swollen granules (Fig. 8B). The highest swelling and area distribution of swollen granules was observed for AHP substituted WMS containing the highest amount of amylopectin. The mean area of the swollen granules of WMS increased up to nine times upon AHP substitution. In untreated starch, 50% of the granules have a surface area between 100 and 250 μm^2, while about 40% of the granules of AHP-WMS have, after swelling, a mean surface of 750–2500 μm^2. AHP-WMS swollen granules are distributed over a broad interval of areas ranging from 100 to 5000 μm^2. Since the amorphous region in the granule is more substituted than the crystalline region (Huijbrechts et al., 2007), this effect might be explained by easier access of the moisture through amorphous regions for AHP-WMS than WMS. Less influence of the AHP substitution on the area of the swollen granules is observed for MS and AEMS starch, respectively. Nonetheless, the mean areas of MS and AHP-MS differs more than a factor four. A shift in area distribution from around 100–250 μm for MS to 250–750 μm for AHP-MS is obtained. Compared to the other native starches tested, AEMS has swollen only slightly at this incubation temperature, due most probably to the high amylose and lipid content that inhibits swelling. Still, the mean area of AEMS after AHP substitution has changed considerably, from 25 to 100 μm for AEMS to 100–500 μm for AHP-AEMS, because of its lower gelatinization temperature (DSC, Table 2).

Table 4
Mean values and standard deviation of swollen starch granules' area heated at 60 °C for 4 h of native and AHP substituted starches

Sample	DS	Mean area (μm^2)	Standard deviation (μm^2)
WMS		120	60
AHP-WMS	0.19	1160	810
MS		130	70
AHP-MS	0.19	570	230
AEMS		90	50
AHP-AEMS	0.17	440	200

Based on these results, we may conclude that AHP substitution induces a higher mean area and broader area distribution of the starch granule by swelling at 60 °C for 4 h and the loss or change of crystalline structure in the granule.

3.7. Behaviour of a droplet of starch suspension under shear conditions: a rheological and rheo-optical study

The goal of this section is to demonstrate a qualitative difference in the behaviour of modified and native starch suspensions under flow.

3.7.1. Steady-state flow of starch suspensions

The flow of starch suspensions with 100% granule volume fraction is shown in Fig. 9. It is clear that the viscosity of non-modified starch is much higher than the one of modified starch. This is due to a low swelling power of native starch granules (Fig. 6) leading to higher granule rigidity and higher polymer concentration in 100% granule volume fraction suspension. All suspensions behave as non-Newtonian fluids: they follow the power law dependence viscosity $\sim$ (shear rate)$^{-n}$ with larger exponents for non-modified starch as compared with modified ones. Maize starch seems to show a plug flow with the exponent close to one.

3.7.2. Rheo-optics: visual observations

The optical micrographs of the droplets of AHP-WMS and AHP-MS granules suspension at 100% volume fraction swollen at maximum and immersed into PDMS are shown in Fig. 10. The initial shape of the droplets of swollen granule suspension is more or less spherical (Fig. 10A and E). Their shape is less regular when the granule is less "soft" because of its decreased swelling power (compare with Fig. 6). Both suspensions of modified starch behave in a similar way: at low shear stresses (σ) the droplets deform (Fig. 10B and F). At increasing shear stress (or

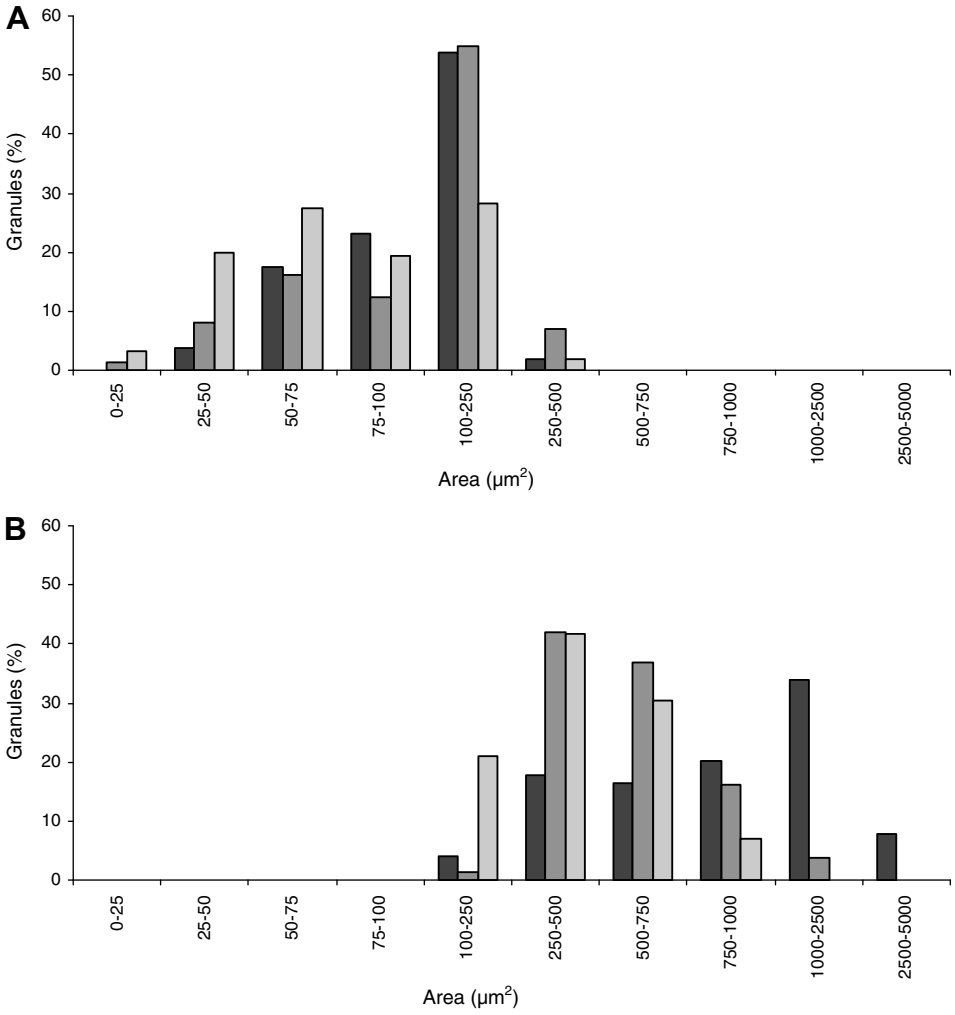

Fig. 8. Average area distribution of granules heated at 60 °C for 4 h in aqueous solutions (A) unmodified ■, WMS; ■, MS; □, AEMS and (B) modified starches: ■, AHP-WMS (DS 0.19); ■, AHP-MS (DS 0.19) and □, AHP-AEMS (DS 0.17).

shear rates, which is the same because PDMS used is a Newtonian fluid in this interval of shear rates) the droplets keep elongating (Fig. 10B and C, F and G) before breaking into two or more smaller ones, approximately of the same size (Fig. 10D and H). During the elongation, the starch suspension moves as a thick paste inside the droplet around the vorticity axis. For the AHP-WMS suspension, rupture occurs at about 500 Pa, for AHP-MS at 1400 Pa. Each newly formed droplet elongates up to breaking under increasing shear. For example, AHP-WMS underwent another break-up into two main droplets at about 690 Pa (not shown). At a fixed shear stress, the droplet breaks down to a certain minimal radius for which no more break-up occurs. Such behaviour is quite similar to the one of a viscous liquid droplet immersed into an immiscible matrix.

Unlike AHP-WMS or AHP-MS, a droplet of a non-modified starch suspension prepared in equivalent conditions (100% volume fraction, maximal swelling) and immersed into PDMS does not have a spherical shape when no shear is applied (see an example of WMS and MS droplets in Fig. 11). It looks like an agglomerate of rigid particles, which is more or less the case. These granules have a much lower swelling power than the AHP modified starches (Fig. 6), they are thus more rigid and much smaller (Table 4) and polymer concentration inside the granule is much higher, this being responsible for the dark colour of the droplet (Fig. 11). Because of particles rigidity, the interfacial tension is playing a smaller role and the droplet is not adapting the spherical shape. The higher is the swelling power, the softer are the particles and the more circular is the shape of the droplet at rest (compare Figs. 10A, E and 11A D, which are ordered with decreasing of swelling power according to Fig. 6). Under shear, the droplet of WMS suspension deforms but does not elongate like the ones of modified starch. A "tail" can be seen as the droplet rotates (Fig. 11B and C). Solvent (water) can be seen in-between the granules, helping to keep them together. The droplet of MS suspension only rotates but does not deform.

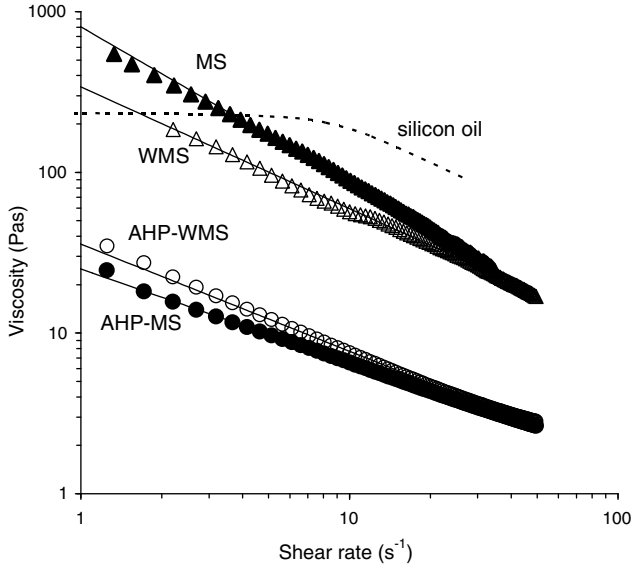

Fig. 9. Flow curves of modified and non-modified starch suspensions with 100% granule volume fraction. Points are experimental data, lines are power law fits with $n = 0.58$ (AHP-MS, DS = 0.19), 0.67 (AHP-WMS, DS = 0.19), 0.74 (WMS) and 0.95 (MS). Dashed line corresponds to PDMS.

3.7.3. Deformation of droplets: comparison between modified and non-modified starches

An example of the evolution of the droplet relative length $L(t,\sigma)/L_0$ (Fig. 10) as a function of strain (shear rate × time, s/s) for AHP-WMS suspension is presented in Fig. 12. As was shown in Fig. 10, the droplet elongates up to rather high values, and at a certain strain (≈140 s.u.) rupture occurs which is reflected by a sharp decrease of L/L_0. The evolution of one of the "secondary" droplet is then followed as a function of strain and a second rupture occurs around 330 strain units or 680 Pa.

The comparison of the evolution of L/L_0, up to the first break-up, for AHP-WMS and AHP-MS starch suspension droplets as a function of strain is shown in Fig. 13. The rupture of AHP-MS droplets occurs much later, or at higher stresses (1370 Pa), than for AHP-WMS droplet (510 Pa). When making qualitative analogies with the deformation and break-up of a liquid droplet in an immiscible matrix (Grace, 1982), for the cases when viscosity of the droplet is lower than the one of the suspending fluid, droplet break-up should occur at lower shear stresses for a fluid with a higher viscosity (so-called Grace diagram) keeping all the other system parameters like the interfacial tension, droplet initial size and matrix viscosity were kept the same. This is what we obtained: both AHP-MS and AHP-WMS suspension viscosities are lower than the one of PDMS (Fig. 9), whereas AHP-WMS viscosity is slightly higher than the one of AHP-MS (Fig. 9) in the region of applied stresses and all other parameters are practically the same. However, even fitting with the classical theoretical prediction, such a comparison remains qualitative and rather superficial because the Grace diagram is made for Newtonian emulsions in the steady-state, which is not the case of starch suspensions shown in Figs. 12 and 13. Further studies are needed for making quantitative conclusions.

The next step was to compare the deformation of the droplets of modified starch suspensions with their native ones. An example is given in Fig. 14. Even initially large WMS droplets do not break-up and seem to show saturation at deformations around 1.8, which are much lower than the ones recorded for modified starch droplets before their rupture (dashed lines in Fig. 14). The deformation of the MS droplet is negligible (data not shown in order not to overload the graph), not higher than 10%, which is within experimental errors.

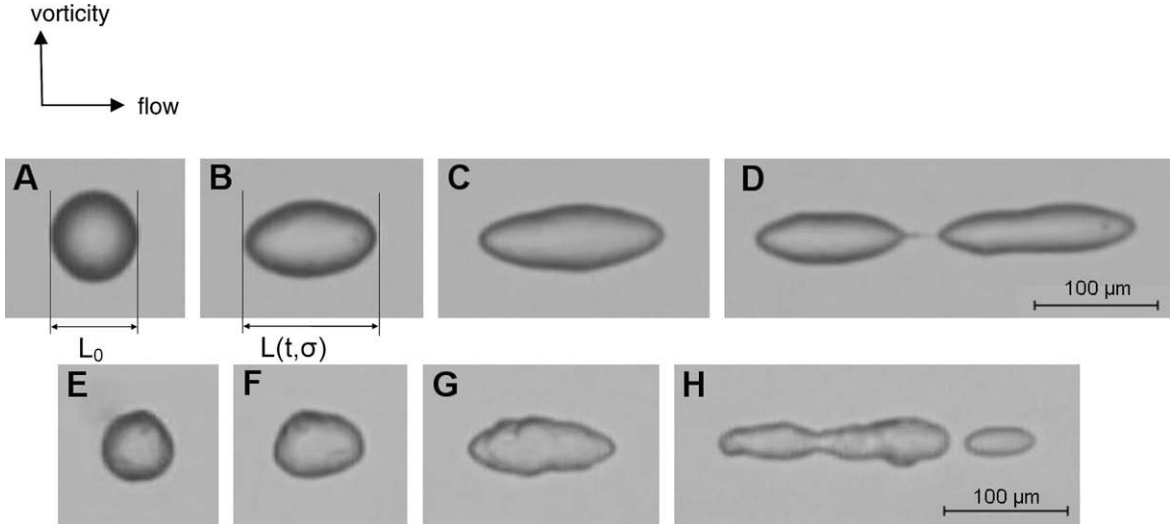

Fig. 10. Optical micrographs of AHP-WMS (A–D) and AHP-MS (E–H) droplets of suspensions of 100% granules volume fraction, deforming in time (t) and under shear stress (σ). AHP-WMS: 0 Pa, initial droplet diameter $L_{\text{AHP-WMS, 0}} = 80$ µm (A); $t = 35$ s, 300 Pa (B); $t = 54$ s, 420 Pa (C) and $t = 67.5$ s, 510 Pa (D); AHP-MS: 0 Pa, initial droplet diameter: $L_{\text{AHP-MS, 0}} = 70$ µm (E); $t = 50$ s, 710 Pa (F); $t = 70$ s, 1070 Pa (G) and $t = 90$ s, 1370 Pa (H). The gap was 900 µm. Flow and vorticity direction in the rotating cell are shown by arrows.

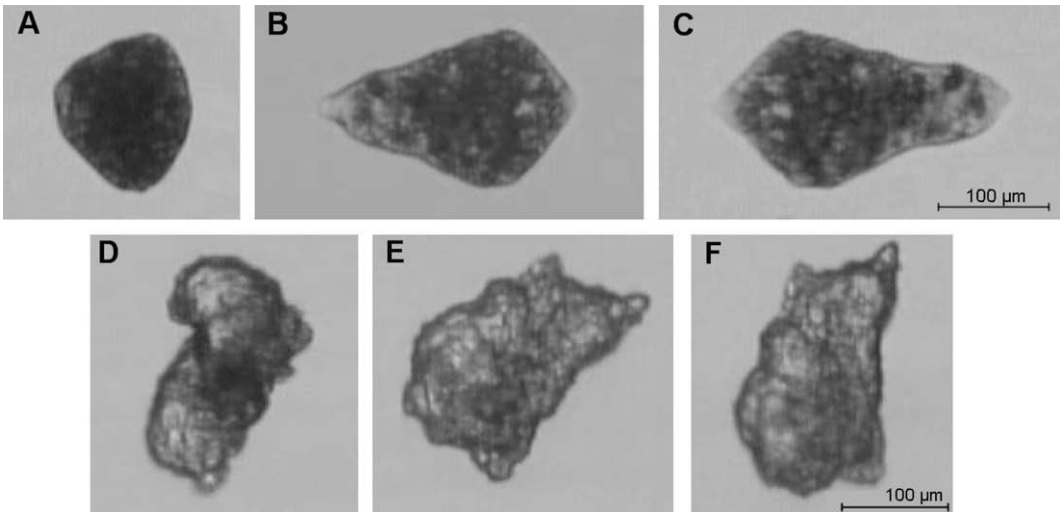

Fig. 11. Optical micrographs of a droplet of WMS and MS suspensions with 100% volume fraction granules, at different shear stresses: WMS at 0 Pa, initial size: $L_{WMS,\,0} = 145$ μm (A); 650 Pa (B) and 1090 Pa (C); the "tail" is visible on the left (B) and right (C) of the picture showing the rotation of the droplet; MS at 0 Pa (D); 830 Pa (E) and 1300 Pa (F). The gap was 900 μm.

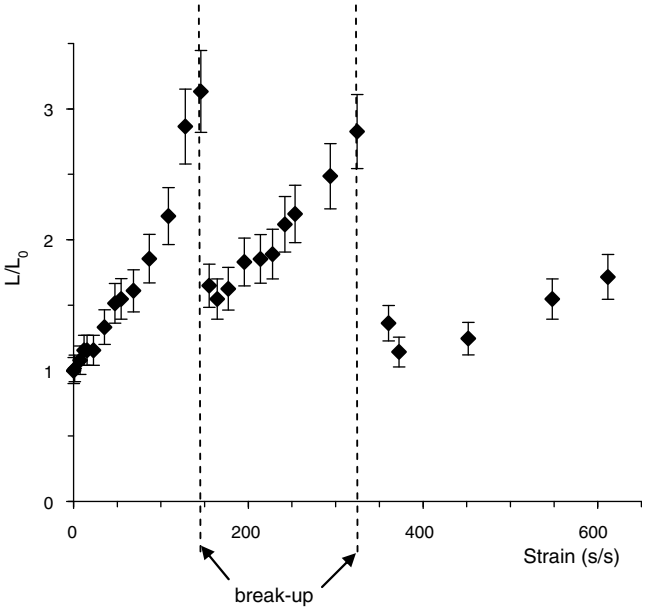

Fig. 12. Evolution of the relative length of a droplet of AHP-WMS suspension (100% granule volume fraction, maximal granule swelling) as function of strain: droplet initial size was $L_{AHP\text{-}WMS,\,0} = 80$ μm, rupture at 510 and 680 Pa is shown by dashed lines, shear rates were varied from 0 to 4 s^{-1}, shear stresses from 0 to 900 Pa.

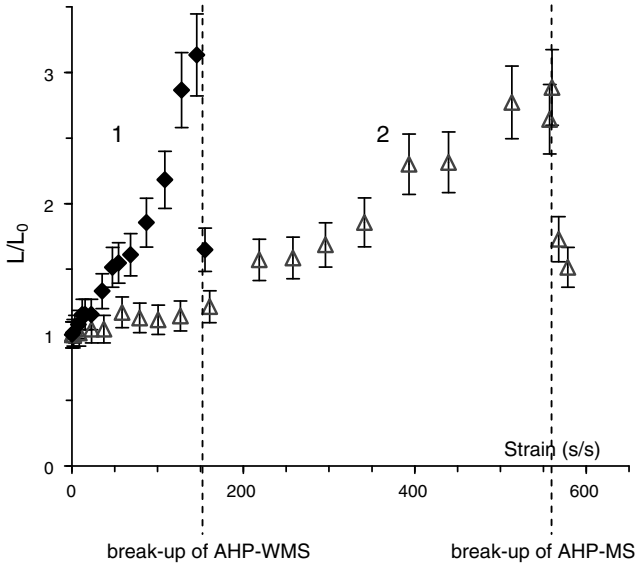

Fig. 13. Evolution of the relative droplet length as a function of applied strain for AHP-WMS (1) and AHP-MS (2) starch suspension droplets, granule volume fraction 100%, granules swollen at maximum, $L_{AHP\text{-}WMS,\,0} = 80$ μm and $L_{AHP\text{-}MS} = 70$ μm. The data for AHP-WMS are the same as in Fig. 12. Shear rates were varied from 0 to 6.5 s^{-1}. The first break-up of AHP-MS droplet occurs at 1370 Pa.

Such a different behaviour of the droplets of modified and non-modified starch suspensions is related to different swelling power of the granules and thus polymer concentration and granule rigidity, the latter governing suspension viscosity. For the case of WMS suspension, its viscosity is still lower than PDMS (Fig. 9). When again making analogies with classical liquid droplets suspended in an immiscible matrix, native starch droplets should break-up at lower capillary numbers than the modified starch droplets, because of higher viscosities of the non-modified starch suspensions and larger droplet size (Grace, 1982). We obtained the opposite result: no break-up was observed for the native starch suspension even at higher stresses and for an initially larger droplet (Fig. 14). Lower capillary numbers mean lower stress at break-up and/or smaller initial droplet size (which does not correspond to our case, as mentioned above), or higher interfacial tension. The notion of the interfacial tension for a suspension with 100% particle volume fraction is a delicate point. It seems that there is some free liquid in-between the granules (Fig. 11B and C) even if suspensions were prepared in such a way that the granules should absorb all water. Is this

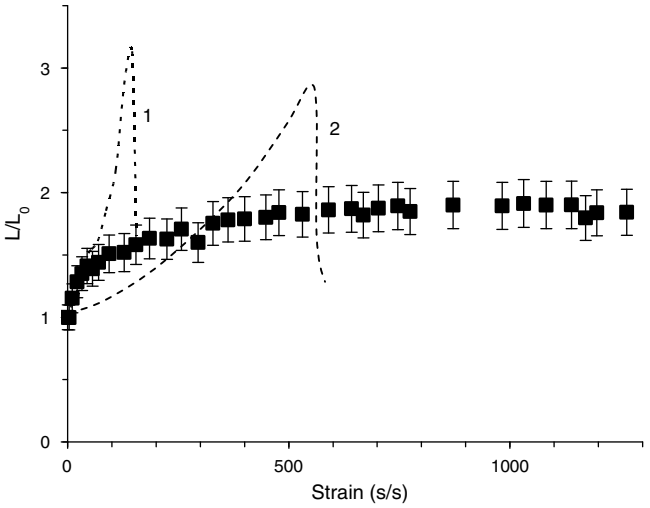

Fig. 14. Comparison of the evolution of droplet suspension of WMS starch with 100% volume fraction, maximal granule swelling (dark points), as a function of strain, with droplet behaviour of AHP-WMS (1) and AHP-MS (2) suspensions before break-up. $L_{WMS,\,0} = 145$ μm, shear rates were varied up to 8.2 s^{-1}, shear stresses up to 1800 Pa.

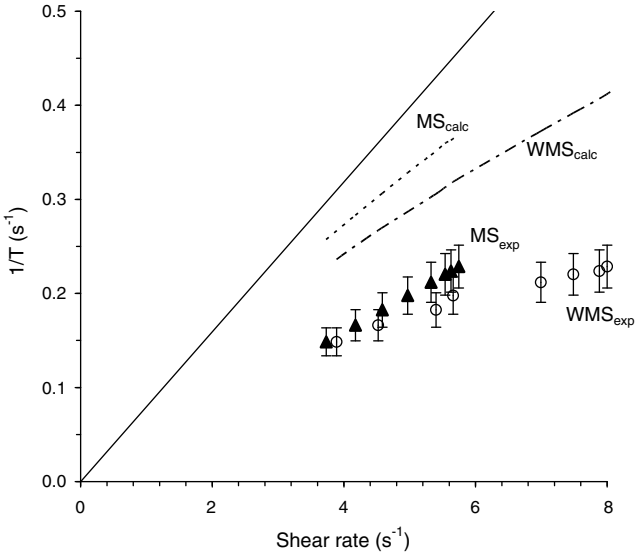

Fig. 15. Rotation period as a function of shear rate for droplets of WMS (open points) and MS (dark points) suspensions. Solid line corresponds to Jeffery law (Eq. (1)); dashed and dashed-dotted lines correspond to calculated dependences (Eq. (2)) for MS and WMS, respectively.

liquid pure water that was left not adsorbed or water or polysaccharide solution released from the granules due to shear? The release of solvent from a swollen synthetic microgel particle under shear has been reported (Vervoort & Budtova, 2005; Zanina & Budtova, 2002). If the liquid between the granules is water, the droplet is not breaking because of the high interfacial tension water/PDMS. This could explain the absence of the break-up of the droplet of native starch suspension.

It was possible to measure the period of rotation of WMS and MS droplets and compare with the approaches developed for a rigid particle rotating in a fluid under shear and for a liquid Newtonian droplet. The results are shown in Fig. 15.

It is known that the rotation period of a rigid spherical particle immersed in a Newtonian fluid is described by Jeffrey's law (1) (Jeffery, 1922) where the period T is inversely proportional to the shear rate γ:

$$T = \frac{4\pi}{\gamma} \tag{1}$$

In the case of a sheared droplet, viscous forces exerted by the suspending matrix induce circulation of the fluid inside the droplet (Bartok & Mason, 1958), and the mean period of its circulation on the droplet surface is given by expression (2):

$$T = \frac{4\pi}{\gamma}\,\frac{p+1}{\sqrt{p(p+2)}} \tag{2}$$

where p is the ratio of droplet to suspending matrix viscosity. The slope of $T = f(\gamma)$ depends on viscosity ratio: it increases with increase of p and reaches Jeffrey law (1) at $p = \infty$.

All experimental points (Fig. 15) fall far below the solid line corresponding to the rotation of a solid particle and below the dashed lines that correspond to the period of liquid circulation in a droplet, the latter calculated taking into account the viscosity of each suspension at the corresponding shear rate from Fig. 9. The fact that experimental data are far from those predicted by Eq. (1) was to be expected: the droplet of non-modified starch suspensions is highly asymmetric and deformable. Asymmetry, inhomogeneity, the non-Newtonian character of suspension viscosity of the droplets studied and their possible viscoelastic behaviour can explain the difference between experimental data and liquid droplet approach.

4. Conclusions

The observed changes in starch properties due to etherification have been described in this paper. In dry granular starch, no appreciable changes in granular form for the three different maize starches are obtained. A high degree of substitution with AHP groups causes a large decrease in starch crystallinity for AHP-WMS and AHP-MS. AHP-AEMS seems to have a slightly better DC, which is confirmed by a higher ΔH_{gel}. The incorporation of AHP substituents in the starch molecules significantly affects their physicochemical properties. All gelatinization temperatures are reduced after modification. Furthermore, the altered pasting properties lead to shear thinning during heating and a better gel network after cooling for AHP-WMS and AHP-MS. The swelling power of all starches increases as DS increases. Similarly, the solubility index of WMS and MS increases as DS increases. Microscopic measurements confirm the swelling capacities of the three starches in order of AHP-WMS > AHP-MS > AHP-AEMS at 60 °C. Granules with increased swelling power induce a desirable change in the flow behaviour under shear, making them interesting for bio-

materials (Seidel et al., 2001). Immersed into PDMS, droplets of AHP modified WMS and MS suspension (100% volume fraction, maximal swelling) break-up into several smaller droplets under shear, whereas the native starches do not elongate, but only form a "tail" or only rotate in the vorticity direction.

Acknowledgments

We thank Jacqueline Donkers for SEM measurements and Dr. Marcel Giesbers for the interpretation of X-ray diffraction spectra. This research was conducted within the framework of the Carbohydrate Research Centre Wageningen, and partly financed by the Ministry of Agriculture, Nature and Food Quality of The Netherlands and the Graduate School VLAG.

References

Altay, F., & Gunasekaran, S. (2006). Influence of drying temperature, water content, and heating rate on gelatinization of corn starches. *Journal of Agricultural and Food Chemistry, 54*(12), 4235–4245.

Ameye, D., Voorspoels, J., Foreman, P., Tsai, J., Richardson, P., Geresh, S., et al. (2002). Ex vivo bioadhesion and in vivo testosterone bioavailability study of different bioadhesive formulations based on starch-c-poly(acrylic acid) copolymers and starch/poly(acrylic acid) mixtures. *Journal of Controlled Release, 79*(1–3), 173–182.

Atwell, W. A., Hood, L. F., Lineback, D. R., Varriano-Marston, E., & Zobel, H. F. (1988). The terminology and methodology associated with basic starch phenomena. *Cereal Foods World, 33*(3), 306–311.

Bartok, W., & Mason, S. G. (1958). Particle motions in sheared suspensions. VII. Internal circulation in fluid droplets (theoretical). *Journal of Colloid Science, 13*, 293–307.

Bhandari, P. N., & Singhal, R. S. (2002). Effect of succinylation on the corn and amaranth starch pastes. *Carbohydrate Polymers, 48*(3), 233–240.

Bhuniya, S. P., Rahman, M. S., Satyanand, A. J., Gharia, M. M., & Dave, A. M. (2003). Novel route to synthesis of allyl starch and biodegradable hydrogel by copolymerizing allyl-modified starch with methacrylic acid and acrylamide. *Journal of Polymer Science Part A: Polymer Chemistry, 41*(11), 1650–1658.

Cairns, P., Bogracheva, T. Y., Ring, S. G., Hedley, C. L., & Morris, V. J. (1997). Determination of the polymorphic composition of smooth pea starch. *Carbohydrate Polymers, 32*(3–4), 275–282.

Cheetham, N. W. H., & Tao, L. (1998). Variation in crystalline type with amylose content in maize starch granules: An X-ray powder diffraction study. *Carbohydrate Polymers, 36*(4), 277–284.

Chen, P., Yu, L., Chen, L., & Li, X. (2006). Morphology and microstructure of maize starches with different amylose/amylopectin content. *Starch/Stärke, 58*(12), 611–615.

Chen, P., Yu, L., Kealy, T., Chen, L., & Li, L. (2007). Phase transition of starch granules observed by microscope under shearless and shear conditions. *Carbohydrate Polymers, 68*(3), 495–501.

Donald, A. M. (2007). Understanding starch structure and functionality. In A. C. Elliasson (Ed.), *Starch in food: Structure, function and application* (pp. 156–184). Cambridge and New York: Woodhead Publishing Limited and CRC Press LLC.

Fadzlina, Z. A. N., Karim, A. A., & Teng, T. T. (2005). Physicochemical properties of carboxy-methylated sago (metroxylon sagu) starch. *Food Chemistry and Toxicology, 70*(9), C560–C567.

Gernat, C., Radosta, S., Anger, H., & Damaschun, G. (1993). Crystalline parts of three different conformations detected in native and enzymatically degraded starches. *Starch/Stärke, 45*(9), 309–315.

Grace, H. P. (1982). Dispersion phenomena in high viscosity immiscible fluid systems and applications of static mixers as dispersion devices in such system. *Chemical Engineering Communications, 14*(3), 225–227.

Huijbrechts, A. A. M. L., Huang, J., Schols, H. A., Lagen, B. v., Visser, G. M., Boeriu, C. G., et al. (2007). 1-Allyloxy-2-hydroxy-propyl-starch: Synthesis and characterization. *Journal of Polymer Science Part A: Polymer Chemistry, 45*(13), 2734–2744.

Jane, J., Chen, Y. Y., Lee, L. F., McPherson, A. E., Wong, K. S., Radosavljevic, M., et al. (1999). Effects of amylopectin branch chain length and amylose content on the gelatinization and pasting properties of starch (1). *Cereal Chemistry, 76*(5), 629–673.

Jeffery, G. B. (1922). The motion of ellipsoidal particles immersed in a viscous fluid. *Proceedings of the Royal Society of London. Series A, Containing Papers of a Mathematical and Physical Character, 102*(715), 161–179.

Jenkins, P. J., & Donald, A. M. (1998). Gelatinisation of starch: A combined SAXS/WAXS/DSC and SANS study. *Carbohydrate Research, 308*(1–2), 133–147.

Ji, Y., Wong, K., Hasjim, J., Pollak, L. M., Duvick, S., Jane, J., et al. (2003). Structure and function of starch from advanced generations of new corn lines. *Carbohydrate Polymers, 54*(3), 305–319.

Kaur, L., Singh, N., & Singh, J. (2004). Factors influencing the properties of hydroxypropylated potato starches. *Carbohydrate Polymers, 55*(2), 211–223.

Kondo, T., Isogai, A., Ishizu, A., & Nakano, J. (1987). Preparation of completely allylated and methallylated celluloses from methylcellulose and cellulose acetate. *Journal of Applied Polymer Science, 34*(1), 55–63.

Lewandowicz, G., Fornal, J., & Voelkel, E. (2001). Starch ethers obtained by microwave radiation – structure and functionality. In T. L. Barsby, A. M. Donald, & P. J. Frazier (Eds.), *Starch: Advances in structure and function* (pp. 82–96). Cambridge, UK: Royal Society of Chemistry.

Li, J. H., Vasanthan, T., Hoover, R., & Rossnagel, B. G. (2004). Starch from hull-less barley. IV. Morphological and structural changes in waxy, normal and high-amylose starch granules during heating. *Food Research International, 37*(5), 417–428.

Liu, H., Corke, H., & Ramsden, L. (1999). Functional properties and enzymatic digestibility of cationic and cross-linked cationic ae, wx, and normal maize starch. *Journal of Agriculture Food Chemistry, 47*(7), 2523–2528.

Liu, H., Ramsden, L., & Corke, H. (1997). Physical properties and enzymatic digestibility of acetylated ae, wx, and normal maize starch. *Carbohydrate Polymers, 34*(4), 283.

Liu, H., Ramsden, L., & Corke, H. (1999). Physical properties and enzymatic digestibility of hydroxypropylated ae, wx, and normal maize starch. *Carbohydrate Polymers, 40*(3), 175.

Matveev, Y. I., Soest, J. J. G. v., Nieman, C., Wasserman, L. A., Protserov, V. A., Ezernitskaja, M., et al. (2001). The relationship between thermodynamic and structural properties of low and high amylose maize starches. *Carbohydrate Polymers, 44*(2), 151–160.

Moorthy, S. N. (2007). Tropical sources of starch. In A. C. Elliasson (Ed.), *Starch in food: Structure, function and application* (pp. 321–359). Cambridge and New York: Woodhead Publishing Limited and CRC Press LLC.

Nicohols, P. L., Hamilton, J. R. M., Smith, L. T., & Yanovsky, E. (1945). Allyl ether of starch. *Industrial and Engineering Chemistry, 37*(2), 201–202.

Nud'ga, L. A., Petrova, V. A., & Lebedeva, M. F. (2003). Effect of allyl substitution in chitosan on the structure of graft copolymers. *Russian Journal of Applied Chemistry, 76*(12), 1978–1982.

Radosta, S., Vorwerg, W., Ebert, A., Begli, A. H., Grülc, D., & Wastyn, M. (2004). Properties of low-substituted cationic starch derivatives prepared by different derivatisation processes. *Starch/Stärke, 56*(7), 277–287.

Rasband, W. S. (1997–2006). ImageJ. Available from: http://rsb.info.nih.gov/ij/. Bethesda, Maryland, USA: US National Institutes of Health.

Rolee, A., Chiotelli, E., & Meste, M. L. (2002). Effect of moisture content on the thermomechanical behaviour of concentrated waxy corn

starch–water preparations – a comparison with wheat starch. *Journal of Food Science, 67*(3), 1043–1050.

Rutenberg, M. W., & Solarek, D. (1984). Starch derivatives: Production and uses. In R. L. Whistler, J. N. Bemiller, & E. F. Paschall (Eds.), *Starch: Chemistry and technology* (2nd ed., pp. 311–366). New York: Academic Press.

Seidel, C., Kulicke, W.-M., Heß, C., Hartmann, B., Lechner, M. D., & Lazik, W. (2001). Influence of the cross-linking agent on the gel structure of starch derivatives. *Starch/Stärke, 53*(7), 305–310.

Shon, K.-J., & Yoo, B. (2006). Effect of acetylation on rheological properties of rice starch. *Stärke/staerke, 58*(3–4), 177–185.

Subramanian, V., Hoseney, R. C., & Bramel-Cox, P. (1994). Shear thinning properties of sorghum and corn starches. *Cereal Chemistry, 71*(3), 272–275.

Tan, I., Flanagan, B. M., Halley, P. J., Whittaker, A. K., & Gidley, M. J. (2007). A method for estimating the nature and relative proportions of amorphous, single, and double-helical components in starch granules by ^{13}C CP/MAS NMR. *Biomacromolecules, 8*(3), 885–891.

Tester, R. F., & Morrison, W. R. (1990). Swelling and gelatinization of cereal starches. I. Effects of amylopectin, amylose, and lipid. *Cereal Chemistry, 67*, 199–203.

Thomas, D. J., & Atwell, W. A. (1999). *Starches*. St. Paul, MN, US: Eagen Press.

Tsai, J. J., & Meier, E. A. (1990). Polysaccharide graft copolymers containing reactive aminoethyl halide group (p. 13). United States: National Starch and Chemical Investment Holding Corporation (Wilmington, DE). US Patent 4,973,641.

Vervoort, S., & Budtova, T. (2005). Shear-induced gel widening and solvent release in the vorticity direction. *Colloids and Surfaces A: Physicochemical and Engineering Aspects, 262*(1–3), 132–138.

Wang, Y.-J., & Wang, L. (2002). Characterization of acetylated waxy maize starches prepared under catalysis by different alkali and alkaline-earth hydroxides. *Starch/Stärke, 54*(1), 25–30.

Whistler, R. L., & Bemiller, J. N. (1997). Starch. In R. L. Whistler & J. N. Bemiller (Eds.), *Carbohydrate chemistry for food scientists* (pp. 117–151). St. Paul, MN, US: Eagen press.

Wilham, C. A., McGuire, T. A., Rudolfhi, A. S., & Mehltretter, C. L. (1963). Polymerization studies with allyl starch. *Journal of Applied Polymer Science, 7*(4), 1403–1410.

Zanina, A., & Budtova, T. (2002). Hydrogel under shear: A rheo-optical study of the particle deformation and solvent release. *Macromolecules, 35*(5), 1973–1975.